J H. Enns
4045 Randall

ENGINEERING RESEARCH INSTITUTE
UNIVERSITY OF MICHIGAN
ANN ARBOR

PROGRESS REPORT

APPLICATION OF DIRECT-RECORDING METHODS TO THE STUDY OF SPARK-SOURCE EXCITATION PARAMETERS IN SPECTROCHEMICAL ANALYSIS OF STEEL

By

J. H. ENNS
Research Physicist

Project M567

LEEDS AND NORTHRUP COMPANY
PHILADELPHIA, PENNSYLVANIA

June 18, 1951

TABLE OF CONTENTS

APPLICATION OF DIRECT-RECORDING METHODS TO THE STUDY OF SPARK-SOURCE EXCITATION PARAMETERS IN SPECTROCHEMICAL ANALYSIS OF STEEL

PART A. INSTRUMENTATION

A 1. Introduction

The application of a ratio recorder to the study of sources was first discussed in the spring of 1946. A preliminary outline of our program appears in an M567 project report, dated October 10, 1946. Previous work with the two-gun oscilloscope led to the belief that direct recording of a spectrum line or the ratio of two lines should be beneficial in the selection of excitation parameters for a particular sample.

Part A of the present report deals with the overall arrangements of our system and certain of its properties. A detail description of the pre-amplifier electronics and automatic switching is contained in an instructions manual prepared for project M807, dated July 5, 1949 (copies of this manual were submitted to Leeds and Northrup at that time). The contents of this manual apply equally to our equipment, except for the multiplier-tube power supply. The voltage supply for our instrument is as described on page 14 of the October 10, 1946, M567 progress report.

A 2. Spectrograph and Photo-tube Assembly

Fig. 1 is a schematic presentation of the optical and electrical signal paths. One portion of the radiation from the source at 6 (analytical gap) enters the spectrograph for dispersion into element lines, while a second portion selectively filtered by the UV filter 1 falls on the receiver 5. A spectrum line enters a particular MT (multiplier tube) housing through the 150 micron exit slit whose effective opening normal to the incoming line is roughly 70 microns. Keeping the entry slit to a 5 mm length reduces the difficulty of paralleling all four exit slits simultaneously with the entry slit. This also reduces to a neglibible amount the effects of spectrum line curvature in the focal plane at the exit slits.

The cylindrical, aluminized mirrors 11 are adjustable from an external position for maximum signal output by its receiver. Setting any one of the MT's on a line is a manual operation and can be repeated to an accuracy of a few microns. Receiver 5 for the reference signal is rigidly mounted on the spectrograph near the entry slit.

Simultaneous to recording the ratio I_x/I_s, a microampere recorder is arranged to record the magnitude of either I_x or I_s. On the charts that follow both records are usually shown, with one appearing directly above the other. The arrangement has often lead towards a more complete interpretation of intensity and ratio behavior. The time in all records is from right to left at a recorder paper speed of 30 seconds to the inch.

A 3. Photo-tube Currents and Radiation Signal Strength

The four 1P28 multiplier tubes presently installed in our system have d-c, dark-current properties as a function of the dynode voltage supply shown in Table I. It is convenient here to arrange them in the order left to right as they appear in the tube mounting. Tube 2 is the only one with an appreciable dark current that also increases in observable amounts with increasing dynode voltage. This tube should preferrably be operated at not more than 78 volts. The other three tubes have comparatively low dark currents

TABLE I

D-C DARK CURRENT OF 1P28 MT'S IN MICROAMPERES

Tubes / Dynode Volts	2	1	4	3
78	.003	.0015	.0055	.002
86	.006	.0015	.0045	.002
95	.015	.0015	.0045	.002
105	.045	.003	.0055	.0025

whose change with increasing Potentials is not detected by the 0.25μA full scale recorder used directly (without preamplifier) in these measurements.

In Table II the μA currents for these same tubes are listed, again as a function of the dynode voltage, when subjected to a low-intensity neon

TABLE II

1P28 MT MICROAMPERE CURRENT
FOR A CONSTANT LIGHT SIGNAL

Tubes / Dynode Volts	2	1	4	3
78	.09	.006	.0075	.0225
86	.18	.011	.0125	.0445
95	.37	.022	.0255	.0875
107	.80	.044	.0515	.1845

light source placed just in front of, and below the spectrographic collimating lens. As above, these are the d-c currents directly recorded on the micro-ampere recorder, but in each case the dark currents from Table I have been subtracted. The currents in Table II allow for a rough comparison between the four receiver systems which must include the multiplier-tube sensitivity exit slit width, and mirror reflective property. Each system has a sensitivity change of about two for successive changes in the dynode voltage.

Properties of the reference band receiver (RCA-935) have not been included because this tube operates at comparatively much higher light intensities and has a negligible dark current under normal operating conditions. While for the 1P28 tubes the d-c signal to noise ratio may be as low as 1:1 under actual conditions the 935 tube is always operated at a much higher ratio. The operating voltage of the 935 tube is 135 volts obtained from two 67-1/2 volts C batteries in series.

A 4. Preamplifier Properties

The purpose of the preamplifiers is to boost the photo-tube output signal to approximately 0.15 volts d-c which is required to operate the ratio recorder and also to improve the signal to noise ratio. In this laborabory brief comparison tests on the Leeds and Northrup vibrator type and our own RC tuned amplifiers resulted in the following observations:

a) The L and N, 120-cycle amplifiers are not satisfactory with the multiple-spark excitation source in that it is difficult to contain within the vibrator-closed-position all the sparks of a given half cycle when this number is greater than two or three.[1] This difficulty was eliminated by operating the amplifiers with 60-cycle vibrators and blocking out alternate half-cycle radiation signals with a synchronous chopper in front of the spectrographic entry slit. In this arrangement 50 per cent of the radiation signal is lost.

b) The main objection to our RC tuned amplifiers is the nonlinear property of the copper-oxide rectifiers in the output stage. This effect has been minimized by introducing appreciable series resistance in the rectifier circuit so that a rectifier resistance change due to change in signal current is not significant in the current range of normal operation.

c) Comparison records taken with the 60-cycle vibrator and RC amplifier showed no observable difference. Both are highly stabilized feedback-type amplifiers which, when properly adjusted, do not cause a distortion in the integrated output of the recorder.

The RC amplifiers are tuned to transmit only the 120-cycle component of a given input signal. This frequency has by far the most intense a-c component in the usual d-c pulsating signals from a spark or a-c arc source operating from a 60-cycle line. By comparison, the analyzed MT dark current shows a uniform frequency distribution in the 0 to 100 megacycle interval. The result is a very much improved signal-to-noise ratio as compared to direct d-c operation.

The overall gain of the RC amplifier is represented by Table III.

TABLE III

RC AMPLIFIER GAIN

Tubes / % Transm.	dc μA 4	dc μA 3	120~μA 4	120~μA 3	Ratio $\frac{120\sim}{dc}$ 4	Ratio $\frac{120\sim}{dc}$ 3
55	.028	.147	94	515	3360	3500
100	.05	.26	172.5	937	3450	3600

These data were taken for two light intensities (with and without 55% neutral optical filter) and for two channels (tube 4 on Mn-2933 and tube 3 on Ni-3101). The d-c currents are the values directly recorded (without preamplifier) from which the dark currents of Table I have been subtracted. The 120-cycle currents have been reduced to zero attenuation at the preamplifier input. From the ratios listed in the last columns of Table III it may be concluded that with the excitation source here employed (5 sparks per half cycle), a 1 μA d-c multiplier-tube current is equivalent to 3500 μA in the output of the 120~ amplifier. This factor changes somewhat with the number of sparks in a half cycle, and in the extreme case of a 60-cycle Hg arc source it is out only 1300. According to these figures a recorded 35 μA-120-cycle current corresponds to a .01 μA multiplier-tube current. This we consider as the lower limit of operation for the overall system. In photographic work a spectrum line of this general intensity can be recorded in about 20 seconds with the same excitation parameters.

A 5. Fluctuations in the Recorded Signal

In the study of excitation parameters from spectrum line intensity (μA-microampere) and intensity ratio (I_x/I_s) records, it is essential to know whether the amplitude fluctuations in these records originate in the excitation source, the spectrograph, the detector or the recording unit. That the I_x and I_s branches in the recording unit (preamplifier and recorder) transmit their input signals without distortion is proven by the constant straight-line ratio obtained from a pair of signals taken from the same detector. In the RC tuned (120cps) preamplifiers the gain of each branch is so adjusted that the common signal ratio is recorded as unity, which means that the overall gain of the system past the detectors is identical for the I_x and I_s branches. These systems fail to be linear (unity ratio is not maintained) for signal intensities below 25 per cent of full scale on μA and for overloads above full scale by a similar percentage. The 3 db ($\sqrt{2}$) step attenuators in the input circuit of each amplifier provide the necessary flexibility for keeping the signal strength within the prescribed limits.

Fluctuations originating in the detector, in this case either a 1P28 multiflier tube or the 935photo-tube employed for the UV band reference signal, are illustrated by the records in Fig. 2. For the Hg arc, it being a comparatively steady source (chart g), charts a, b, and c show that the ratio fluctuations agree in phase and amplitude with the numerator intensity signal simultaneously recorded on the microampere recorder. This particular MT has a d-c dark current of .005 μA and, according to chart a, when the signal current exceeds this current by a factor 10^3, the tube effects become negligibly small.

However, as in c, when the signal current exceeds the dark current by a factor of only 10, statistical variations in the tube cause a spread of as much as 10 per cent from the average (refer to the indicated recorder scale on each chart).

Charts d, e, and f, taken with the same pair of receivers as before, show the dual effects of receiver background and light signal fluctuations. Comparison of charts h and g proves that spark source excitation is far less steady in time than the Hg arc. Even so these records show that if the Ni-2545 line had been of sufficient intensity to give the 8μA output obtained from the Hg line, the ratio records in a and d would appear to be comparable. As it is, the ratio in d corresponds more nearly to b, the two runs in which the d-c signal currents in the MT tube are nearly alike.

The two Ni lines, whose ratio and intensity records are illustrated by charts a, b, and c of Fig. 3, originate from the same upper atomic energy level. Since they are high-energy spark lines, which are essentially free from self-absorption, the ratio of these two lines should be independent of changes in excitation parameters. That this is so is shown in these charts, where, for example, the large intensity dip in a cannot be detected in the corresponding ratio above it. Here again the amplitude of the fine structure increases with a decreasing light signal, indicating that this is a property of the 1P28 tubes. The optical system including the spectrograph and the small convex mirrors in the photo-tube housing do not introduce signal distortion that cannot be erased in ratio measurements. This is not necessarily so in arc source excitation where the lateral displacement of radiating vapor clouds is appreciably greater than in a smooth-running spark source.

The charts to the right in Fig. 3 show the 2913 Ni line the same as on the left and also its ratio with respect to the band. The only significant difference between the left and right ratios is that the line pair ratio assumes an average value that is constant from the start, while the line-to-band ratio increases with time (even more so than shown here when recorded during the initial 10 seconds not shown). This is not a property of differential evaporation, since all radiation is due to the single element, Ni. The ratio rise occurs because in a band both arc and spark lines contribute to the total radiation and the lower energy arc lines have a relatively higher initial intensity.

It may here be summarized that short duration fluctuations observed in the intensity records are due to actual fluctuations in the radiation signal leaving the analytical gap and that these appear as superimposed on the statistical fluctuations of the multiplier tube. In a ratio record the fluctuations originating at the source arc cancelled out, while the MT dark current effects remain. Sample records show that it is desirable to operate with spectral intensities that will yield a signal-to-dark-current ratio of at least 10:1.

PART B. SPARK SOURCE EXCITATION PARAMETERS FOR FERROUS METAL ANALYSIS

B 1. Introduction

With the new Leeds and Northrup scanning-type spectrometer an analysis of a single element is obtained in a few seconds. When the integration time is this short, it is important that the ratio time-of-wait curve is reasonably constant. For a specific sample the trend of these curves may be sharply affected by a change in sample shape, analytical gap spacing, or electrical discharge parameters. It is convenient to group these under the common heading of excitation parameters. A study of the time-of-wait curves below will show that the problem is not just one of excitation--but also includes sample vaporization.

The information here presented was obtained from the study of spark-source excitation parameters for low-alloy, tool, and stainless steels. With the spark source one can avoid overheating of the sample, as shown by local crater formation. Sample deformation to the point of visible cratering invariably causes violent fluctuations in the intensity and ratio.

B 2. Sample Shape

A common practice in metallurgical analysis by spectrochemical methods is to obtain the sample in the form of two short pins of about an 1/8-inch to 3/8-inch diameter. The 7/32 inch pin is a diameter commonly used, probably because it approximates most nearly the 5 mm size in the metric system. The exact diameter is, however, of considerable less importance than the shape to which the two opposing pin ends are prepared for sparking. At least we find this to be true with steels for which the thermal conductivity is low compared to copper or its alloys. Shaping the ends is one way of controlling the rate of sample evaporation. In addition the excitation properties in the discharge are altered so that one observes a 5 to 10 per cent increase in the common element ratio of spark-to-arc lines for a change in cone angle from 130° to 150°. The overall effect is illustrated by Fig 1 and 1a. Each record is of a 60-second run with freshly prepared pins and without preexposure.

In the case of flat pins (equivalent to 180° included angle), due to electrical properties, the discharge prefers to strike from the outer periphery edge. One disadvantage of this is the comparatively large lateral movement of the discharge, thereby introducing noticeable fluctuations in intensity and ratio due to optical-path variations. More important are the effects from differential evaporation as the discharge, quite unsymmetrically in time, samples around the edge. The specimen temperature at the point of sampling continues to increase, as is evidenced by a rising intensity. Increasing the discharge-circuit inductance and/or the number of sparks per unit time, reduces the preference for the outer edge. The discharge is caused to strike more often from the inner flat area. By this means, however, it has not been possible to obtain the desired time-of-wait curves.

Shaping the electrodes to a natural dome, as prescribed by Kaiser[2,3] has the electrical effect that all points on the approximate spherical zone area become points from which the discharge may strike with equal probability. The objection to this pin-shape is that it requires a rather long time for the elements of different boiling temperature to stabilize. Here too, the local temperature of the sampling point is increasing.

When the shape of a pin is that of a cone of 160° included angle or less, the cone apex becomes a preferred point from which the discharge strikes. At 160° the cone is still quite flat and the discharge covers a large portion of the total area. Decreasing the angle concentrates the discharge at the apex. The local temperature and sample vaporization decrease with time. The maximum rate of sample vaporization comes at the beginning, continually decreasing as the apex burns away. The relative rate at which the various elements are vaporized is a constant almost from the start. For the 130° cone the ratio reads 67.5, and this value is only slightly affected by a $\pm 10°$ change in the angle. We have noticed that the ratio is noticeably altered, by as much as 10 per cent, when the cone's lateral elements are not straight lines up to the apex. A lathe-cutting method is recommended for accurate coning. When the sample is too hard for cutting, a tool-post grinder in combination with a lathe may be used. In any case, it is important to check the coning method employed with the reproducibility of the results.

If the steel sample is in the form of a flat, we have used a pure Fe pin as counterelectrode. The counterelectrode when pointed to a 110° cone, will confine the sampled area to a minimum (approximately 2 mm cross section with a low-inductance source). The intensity and ratio records for this sampling method are shown in Fig. 7. The best ratio in these records is not nearly as stable as for the 130°-double cone method.

B 3. Analytical Gap Spacing

For spark source excitation the practical analytical gap spacing is anywhere from 3 to 5 mm. The effect that this spacing has upon the intensity and ratio is shown in Fig. 5. The overall intensity increases with the spacing because of the increased energy dissipation in the gap. It is apparent here that while a 1 mm change in spacing causes an intensity change of about 15 per cent, the ratio is changed by perhaps 1 per cent. Changing the spacing to greater extremes (2 or 6 mm) causes a more pronounced effect on the ratio. Standard practice is to use a fixed spacer (3 or 4 mm), and according to these results this method is sufficiently accurate.

B 4. Electrical Parameters

The electrical properties of a transient spark are fixed by the discharge voltage, V, the capacitance, C, the discharge circuit resistance, R, and inductance, L. With the air interrupter source there is the additional choice in the number of sparks per unit time as shown on the oscilloscope screen. The thermocouple ammeter serves as a convenient indicator for resetting the interrupter gap spacing to obtain the same breakdown voltage, V. The rate at which energy is dissipated in the analytical gap is a function of these variables and may be approximated from the expression

$$W = 1/2 \left[1/2 \, CV^2 n - I_2^2 \, R_2 \right] , \qquad \underline{1}$$

where n is the number of transients per second, C the capacitance in farads, V the breakdown voltage, I_2 the high-frequency amperes, and R_2 the ohmic resistance of the discharge circuit (total resistance exclusive of the gaps). In a two-gap system, as with the analytical and the single interrupter gap, the energy divides approximately equally between the two (the main assumption being that the gap spacings are about the same). This is the origin of the 1/2 factor in front of the brackets. The electrical properties of the transient spark have been described in greater detail elsewhere [3,4,5,6].

In Table IV are listed three sets of electrical parameters, the computed W in watts and the recorder-integrated intensity of the reference band

TABLE IV

Source	Sparks h.c.	C (μ f.)	L (μ h.)	R_2	I_2	K.V.	W	Int.
S IV	4	.002	15	2.1	5	15.5	31	33
SS 4	3	.006	7-1/2	1.1	10	14	51	68
SUC	2	.008	5	2.5	10	19	43	53

(2300-4000 A°) direct without RC preamplification. While there is some doubt in the computed W, nevertheless the accuracy is sufficient to show that relative intensities are in the same ratio to each other as the corresponding watts. This is what one would expect, for both, watts and intensity are similarly integrated quantities of cyclic peak values.

The SUC source parameters in Table IV are those now in use at Universal Cyclops with their photographic installation (there is some disagreement in V, in that we measure 19,000 and they 20,000 volts for a 10-amp. current). The SS 4 source is the one set up at the University of Michigan for low-alloy steel analysis with direct recording instruments. Both sources are operated without added inductance, 7-1/2 μh residual at U. of M. and 5 μ h at UC. The intensity of radiation with cone-shaped electrodes is in each case a decreasing characteristic of the type shown in the lower right-hand trace of Fig. 6. The ratio of element line to band is of the desired constant value shown by the upper trace at the right in this figure. Examining the burn following a 60-second sparking it is observed that the apex of the original cone on each pin is burned away to an altitude of 2/10 to 3/10 mm. The circular area of the final burn is sharply defined by a blackish brown oxide ring of from 1 to 1.3 mm diameter. The volume consumed in the 60 second sparking period is about 1 mm^3 of material. With the SUC source the oxide ring is noticeably darker and more sharply defined than with the SS 4 source.

4a. Inductance effect.--Amongst spectoscopists in the steel industry it is a known fact that increasing the inductance reduces the background radiation, while decreasing it results in higher precision. Since in many laboratories the range of concentrations is well above the troublesome background, the habit is to operate with only the residual inductance (5 to 10μh). Fig. 6 shows the effects upon intensity and ratio when the inductance is varied from a residual of 7-1/2 μh to a total of 30μh. Obviously, the ratio obtained with the 7-1/2μh source is the best for analysis with the scanning spectrometer. An interesting feature in these records is that, as the inductance is increased, the intensity peak at the beginning decreases. At 30μh the intensity is a rising characteristic similar to that for a minimum inductance source and domed electrodes (Fig. 4). An inspection of the sample pins at the various inductance operations shows that the higher inductance causes the discharge to spread, and the heavy oxide ring is not formed with 30μh as is true at 7-1/2μh.

Fig. 7 shows the comparable results for the point-to-plane method. Again the intensity and ratio look best with the low inductance. It now takes 45 to 50 seconds for the ratio to stabilize. The reason for this is that the sampling area covered by the discharge on the flat is not confined (about 2 mm diameter) until a heavy oxide ring is formed. In the case of two cones the discharge is confined to the apex by the sharpness of the points, and as these burn away, the burn is restricted to a 1 to 1-1/2 mm cross section by the oxide ring formed around it.

When the sample (coned pins) is a low-alloy or tool steel (not containing more than several per cent Ni) either the SUC or SS 4 parameters at minimum inductance will result in ratio curves of the type shown at the right in Fig. 6. However, when the sample is a high Ni stainless-steel alloy (Ni above 8 or 9%), local overheating as evidenced by crater formation becomes a problem. In such cases the first approach is to reduce the energy input into the analytical gap. But even the much lower energy of the S IV source is enough to crater a coned stainless-steel sample when the inductance is low. In Figs. 8 and 9 the inductance effects for this case are shown when the cone shapes are 140° and 130°, respectively. The best ratio is obtained when the inductance is just enough to spread the discharge events in the early stages so that the intensity increases as shown in the 12-1/2μh run with the 140° cone and the 15μh run with 130° cone (a flatter sample shape aids the spreading so that a lower inductance may be used). The high Ni alloys have a thermal conductivity essentially one half that of the other steels, and perhaps due to this they tend to crater when successive discharges are concentrated to a small area. We have not always succeeded in reproducing the time-of-wait curves for a given inductance with stainless-steel samples and intend to study this behavior further.

The results show that inductance in the spark circuit may or may not be desirable, depending in these cases on the type of sample. A change of a few microhenries is here far more important in its effect upon the distribution of the discharges, and therefore in sampling, than the effect upon background or relative spectral intensities (arc vs. spark lines).

4b. Spark-circuit resistance.--The residual ohmic resistance of the discharge circuit is considerably less than one ohm (0.1Ω at the U. of M. source). The effect of adding to this resistance in half-ohm steps is shown in Fig. 10. Most noticeable is the decreasing intensity with increased resistance (note the multiplying factors below each curve). Adding or subtracting a half ohm to the 1 ohm of the SS 4 source decreases or increases the intensity by about 35 per cent while the ratio changes only about 3 per cent. There is no apparent change in the general shape of the intensity curve nor in the oxide ring formation, as was noticed with a changing inductance. The distribution of the discharge on the cone's apex is not noticeably affected. The principal function of the resistance is to adjust the energy input to the analytical gap.

4c. Capacitance and voltage.--The most noticeable spectral effect of a change in capacitance is that the overall intensity is changed. One reason for this is that the total energy input is proportional to C according to $1/2\ CV^2$. It is possible to keep the total input constant by a readjustment of V. However, there is the second effect, which is that the spark gap resistance is proportional to $\frac{1}{V}\sqrt{\frac{L}{C}}$. This causes a shift in the fraction of total energy dissipated in the gaps and in the ohmic resistance, R_2.

In Fig. 11 the effects upon intensity and ratio are illustrated when C and V are varied so that the 10-ampere current of the SS 4 source is maintained. While the general intensity is changing for reasons stated above, there is in this case no radical change in the shape of the intensity curves. Also, the integrated ratio is nearly constant, although the peak-to-peak fluctuations appear to be a minimum with the standard SS 4 source at .006 μf.

4d. Sparks per half cycle.--Varying the number of sparks per half cycle between 2 and 4 for the SS 4 source in which the current is kept constant at 10 amperes by adjusting V, results in no apparent change in the ratio and intensity curves. The results are quite similar to those of Fig. 11. When the capacitance is reduced to permit a comparatively large number of sparks (12 to 15 per half cycle), the distribution of the discharges is no longer concentrated near the apex of a cone nor around the outer periphery for a flat pin. The sampling in these cases is difficult to stabilize, and as a result the peak to peak fluctuations increase.

With stainless-steel samples the tendency to crater is reduced if the interval between sparks is increased. For example, in a rectified charging system a single spark at alternate half cycles may not cause cratering, while at lower energy multiple-break, unrectified-operation cratering will start.

B 5. Internal Standard

In quantitative analysis the need for an internal standard is well known, and its advantages have been illustrated by the preceeding records. In most cases shown, a given parameter change caused an appreciable intensity change, while the ratio of element line to internal standard was either not at all, or but slightly, affected.

In the photographic technique a spectrum line usually serves as the internal standard according to the general principles first outlined by Gerlach and Schweitzer.[7] In a German Patent (No. 664,233), August, 1938, J. Heyes proposes the use of total undispersed radiation reflected from the incident face of the dispersing prism as an internal standard signal for the photoelectric technique. With the Leeds and Northrup scanning spectrometer we employ as reference signal a selected undispersed wave-length band separated from the total radiation by absorption filtering. In the following some comparison data are presented in which we have employed different internal standard signals.

The ratio and intensity curves in Fig. 12 do not show any particular advantage of one reference signal over another. Similar results are obtained with an Fe arc line as reference. In general, if at all noticeable, the ratio of element line to the 2300-4000 A° band shows the minimum peak-to-peak fluctutations.

It is a logical assumption that in routine operation of the air-interrupter-type spark source the least certain electrical parameter is the discharge voltage, V. That is, the operator is instructed to make the final adjustments by resetting the interrupter-gap spacing to give the desired high-frequency I_2 current. Figs. 13, 14, and 15 show the effect upon the ratio in which different reference signals are used and where exaggerated changes in the breakdown voltage are introduced by altering the interrupter-gap spacing. (In practice, with the r-f ammeters employed in the Leeds and Northrup sources, it is not likely that a 10-ampere setting would need to be off by more than ± 0.2 amperes). The ratios in these figures have all been reduced to the common scale of 100 at the 9-ampere-source operation. The results show first that for Cr and Si the ratio tends to increase, while for Mo there is a decrease as the current is increased from 9 to 11 amperes. Also the ratio with respect to the 2300-4000 A° band (employed in the L and N direct-reading spectrometer) shows an almost consistent minimum ratio change for each of the three elements. While these results are in the desired direction, the discrepancies that do appear and the reasons for the more favorable ratio from the 2300-4000 band are far too complicated functions of evaporation and excitation to be explained here. It is hoped that additional data can be obtained in the near future to clarify this picture. It may not be possible to obtain the necessary information from integrated intensity measurements, and the instantaneous records of an oscilloscope may be required[8].

SUMMARY

In this study of excitation parameters for steels it is shown that a normal change in some of the parameters results in a change in the general shape of the intensity curves, while a change in certain others affects primarily the magnitude of the intensity. A change in the shape has a more pronounced effect upon the ratio (element line to internal standard) than only an intensity change. Spark circuit inductance, the number of sparks per half cycle, sample shape, and gap spacing contribute to the character of the discharge in such a way that the surface area and depth of sampling may be varied considerably. The other parameters appear to contribute more to the total energy than to the distribution of discharges on the sample surface. At present we feel that analytical reproducibility depends upon the constancy in the manner of sampling (differential evaporation) as well as upon excitation. In all cases, it is important not to overheat the sample with excessive gap energy.

Low-alloy and tool steels are similar and may be excited with identical parameters. The stainless steels can only be run with comparatively low-energy excitation parameters, which must be selected to distribute the sampling area.

Our immediate program is to continue this study. In particular, we propose to check the inability of reproducing time-of-wait intensity curves when the inductance is varied. Unknown at present are the relative analytical reproducibility figures for minimum-inductance sources as compared to small added inductance operation. We plan also to check more thoroughly the comparative merits of the different internal standard signals. Before continuing this phase of our program, a short report on spectral interference in high-concentration analysis will be prepared.

REFERENCE

1) M 567 Project Report, page 32, October 10, 1946.

2) M 567 Project Report, page 1, June 24, 1947.

3) H. Kaiser, Spectrochim. acta, 2, 258 (1942).

4) M 567 Project Report, July 3, 1945.

5) H. Kaiser and A. Wallraff, Ann. d. Physik, 34, 297 (1939).

6) J. H. Enns and R. A. Wolfe, J. Opt. Soc. Am., 39, 298 (1949).

7) W. Gerloch and E. Schweitzer, Foundations and Methods of Chemical Analysis by the Emission Spectrum. London, Adam Hilger, Ltd., 1931.

8) G. H. Dieke, ASTM Special Technical Publication, No. 76, 1948.

FIG. 1 SCHEMATIC DIAGRAM OF OPTICAL AND ELECTRIC SIGNAL PATH

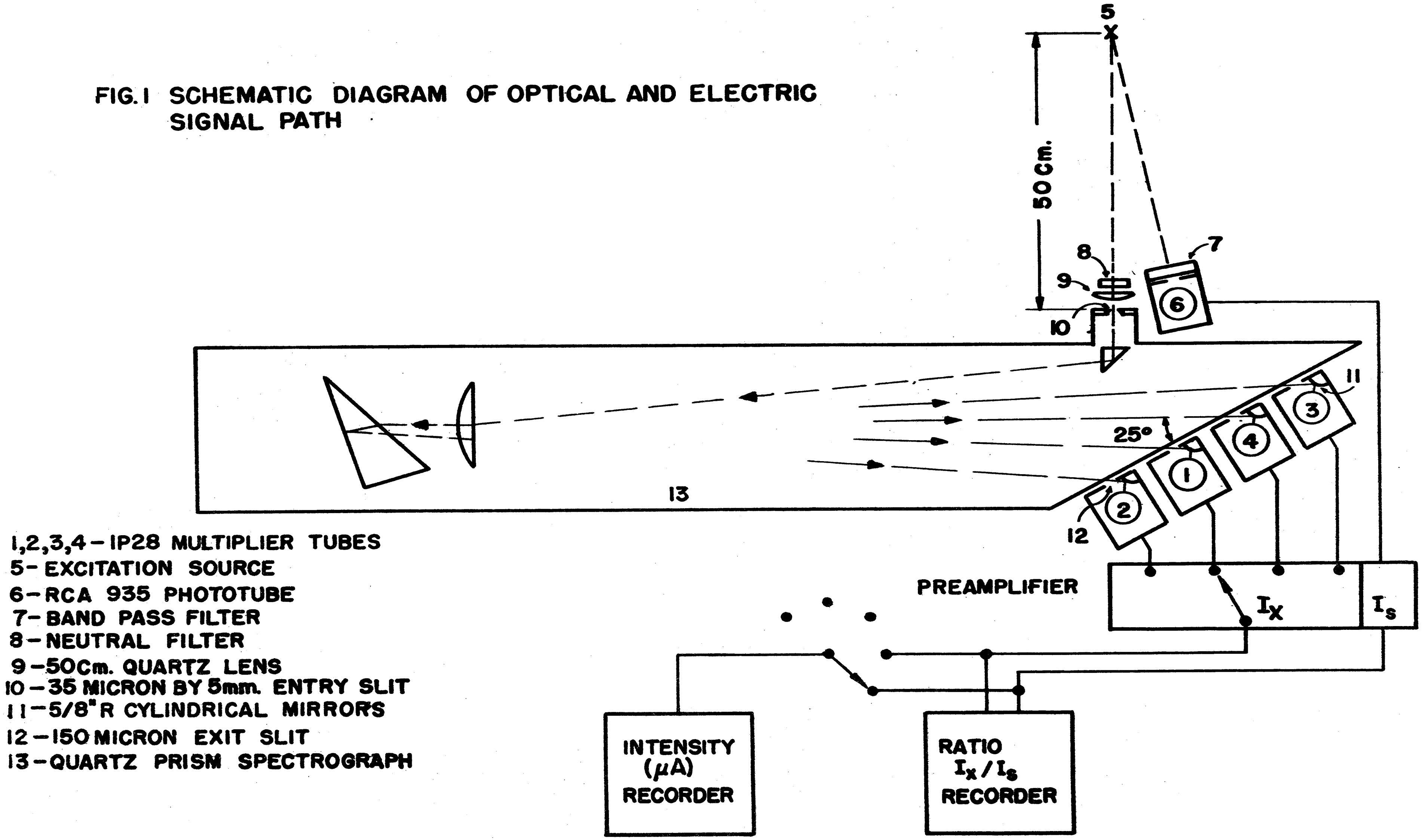

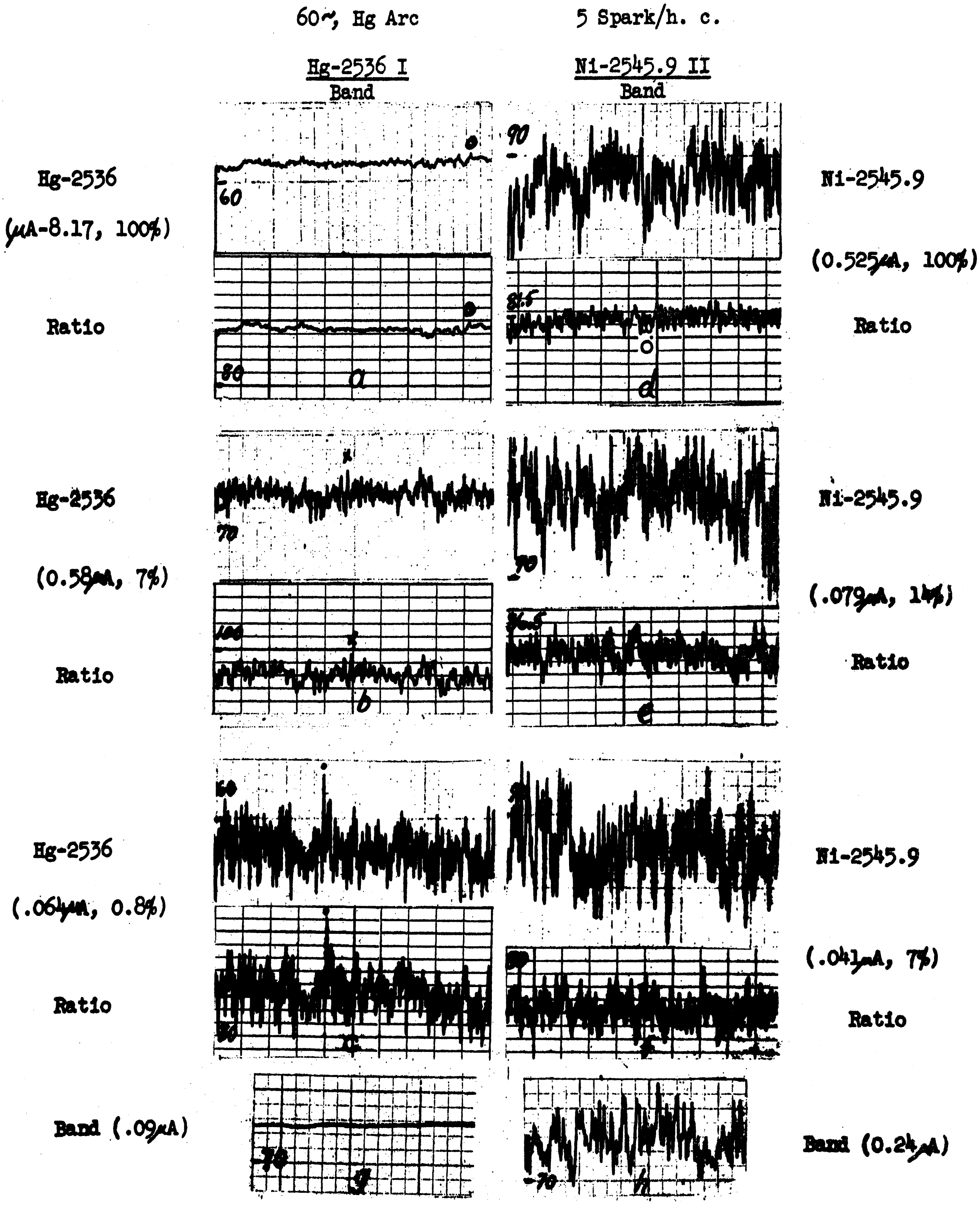

Fig. 2. Ratio of line to band (2300-4000A°) as a function of radiation intensity. μA value is direct current photo-tube current. Per cent value is approximate transmitted radiation through neutral filter at entry slit. No-2 tube at 78 volts on each dynode.

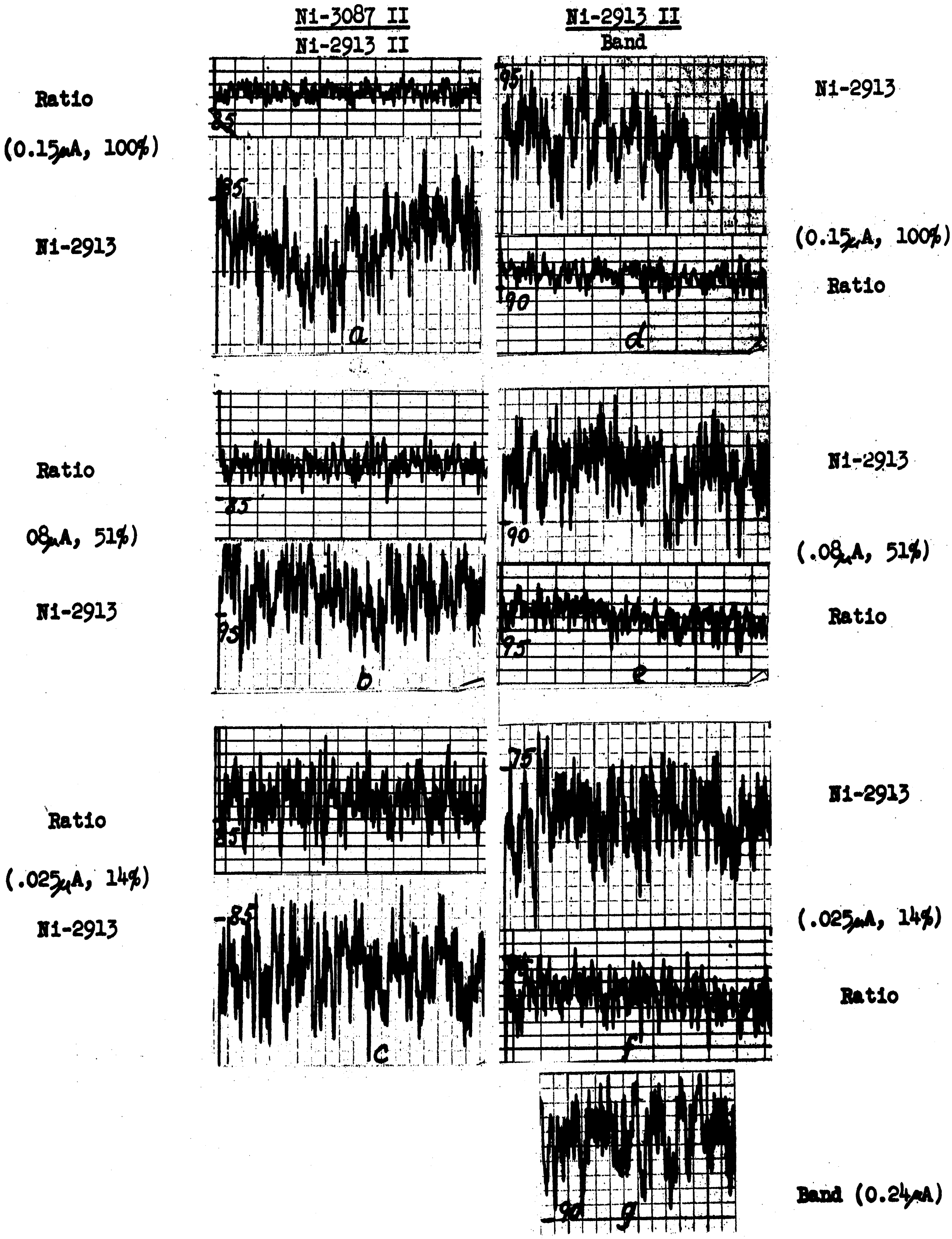

Fig. 3. Ratio of common origin line pair and ratio of line over band (2300-4000A°) as a function of radiation intensity. µA value is integrated photo-tube current. Per cent value is approxmate transmitted radiation through neutral filter at entry slit.

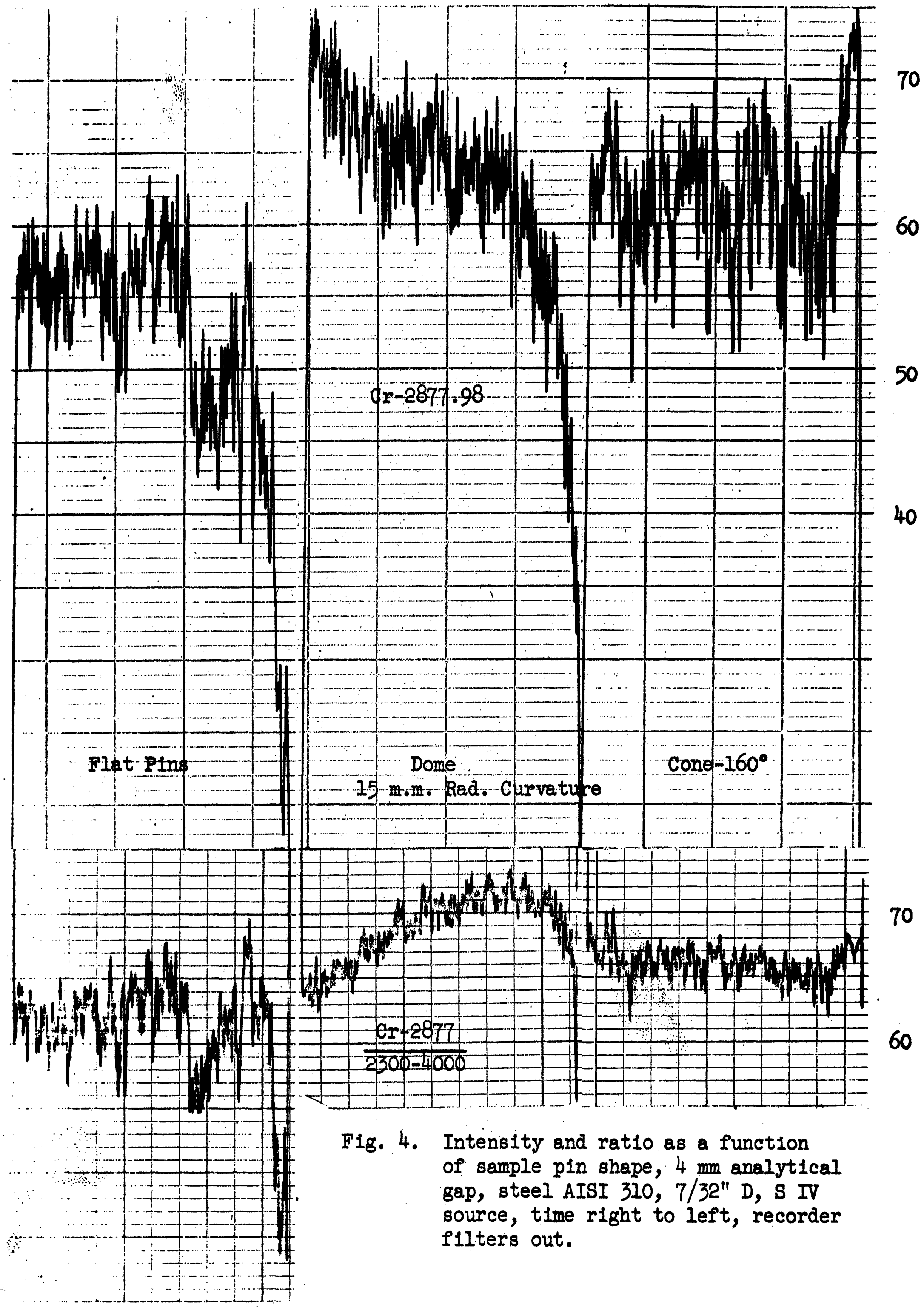

Fig. 4. Intensity and ratio as a function of sample pin shape, 4 mm analytical gap, steel AISI 310, 7/32" D, S IV source, time right to left, recorder filters out.

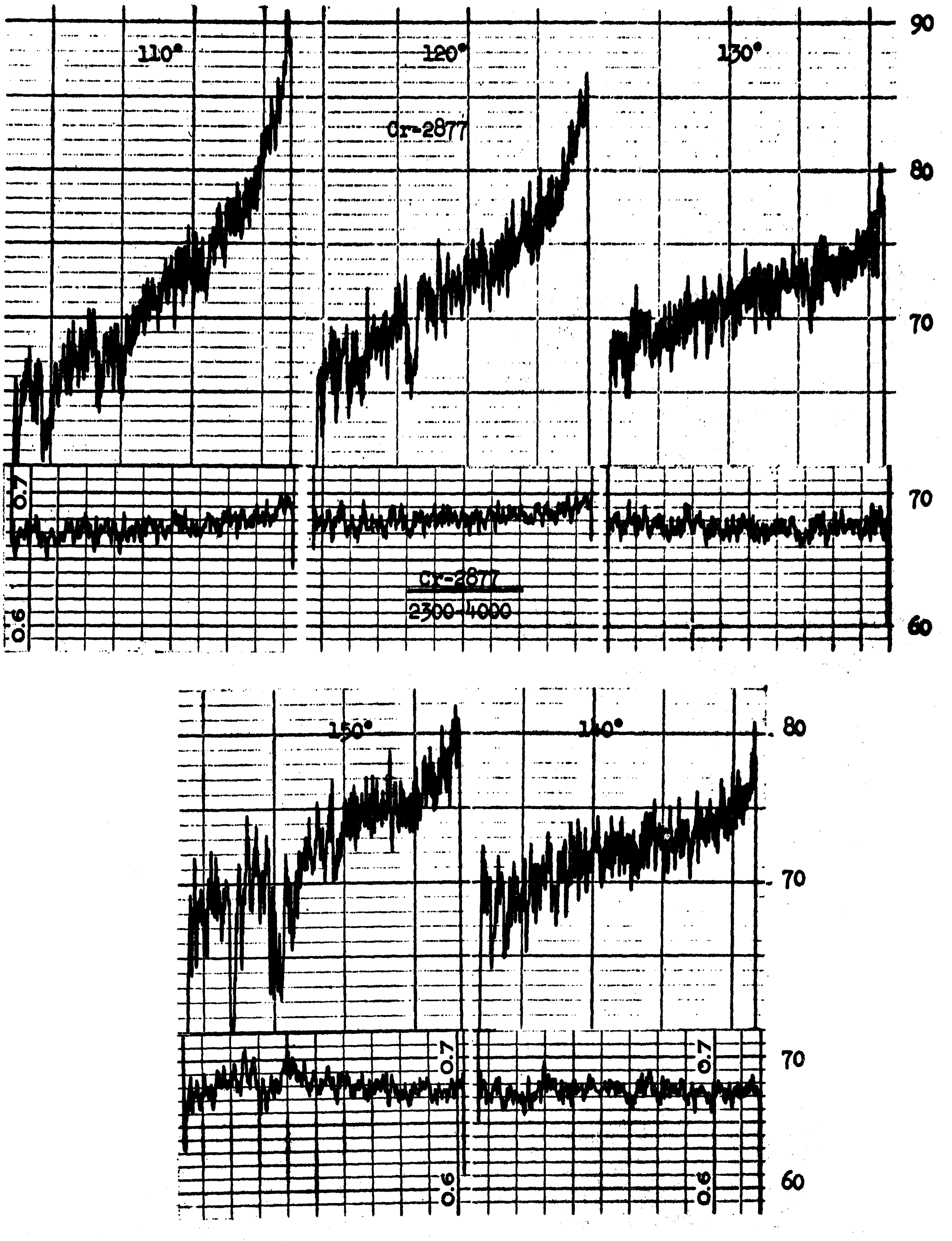

Fig. 4a. Intensity and ratio as a function of sample pin shape continued from Fig. 4.

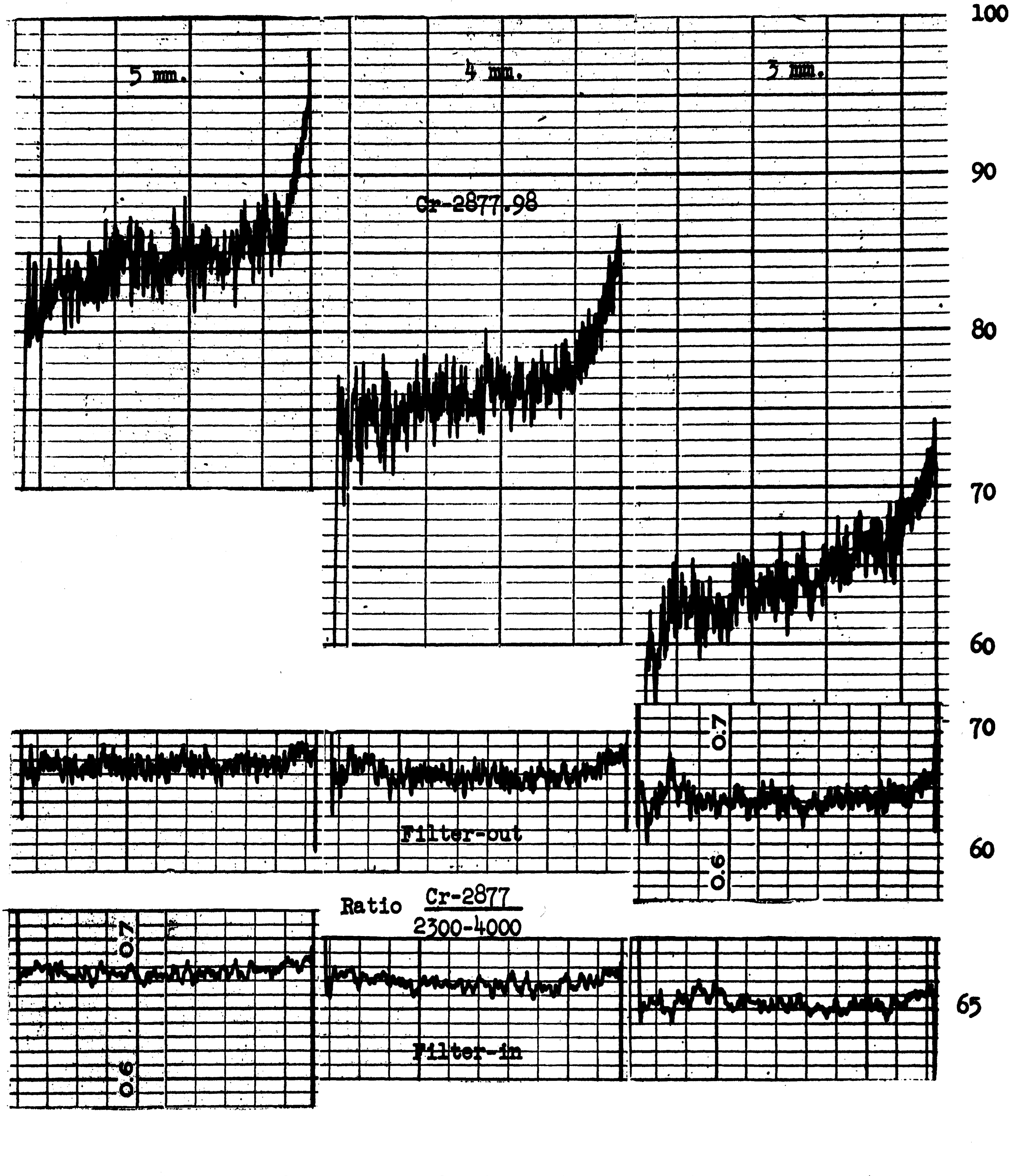

Fig. 5. Intensity and ratio as a function of analytical gap spacing. Stainless steel AISI 310, 7/32", 140° cone. Spark source S-IV. Time from right to left, 60-sec exposures without preexposure. Recorder filters out, ratio taken simultaneously with Cr line intensity above.

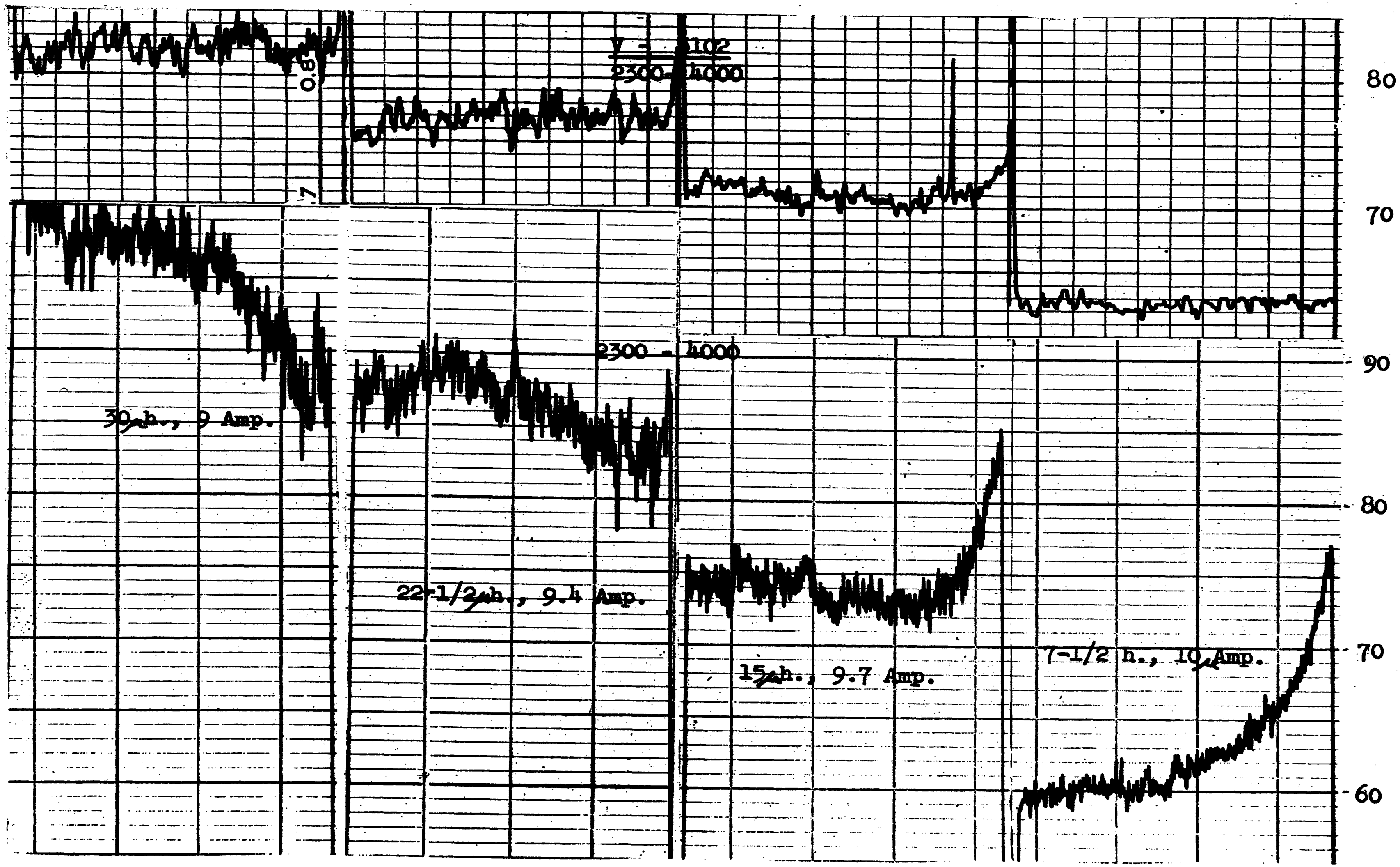

Fig. 6. Ratio and intensity as a function of spark circuit inductance. SS-4 source with increasing inductance. 7/32" D. Motung tool steel pins (1.13% V), 130° cone, 4 mm gap.

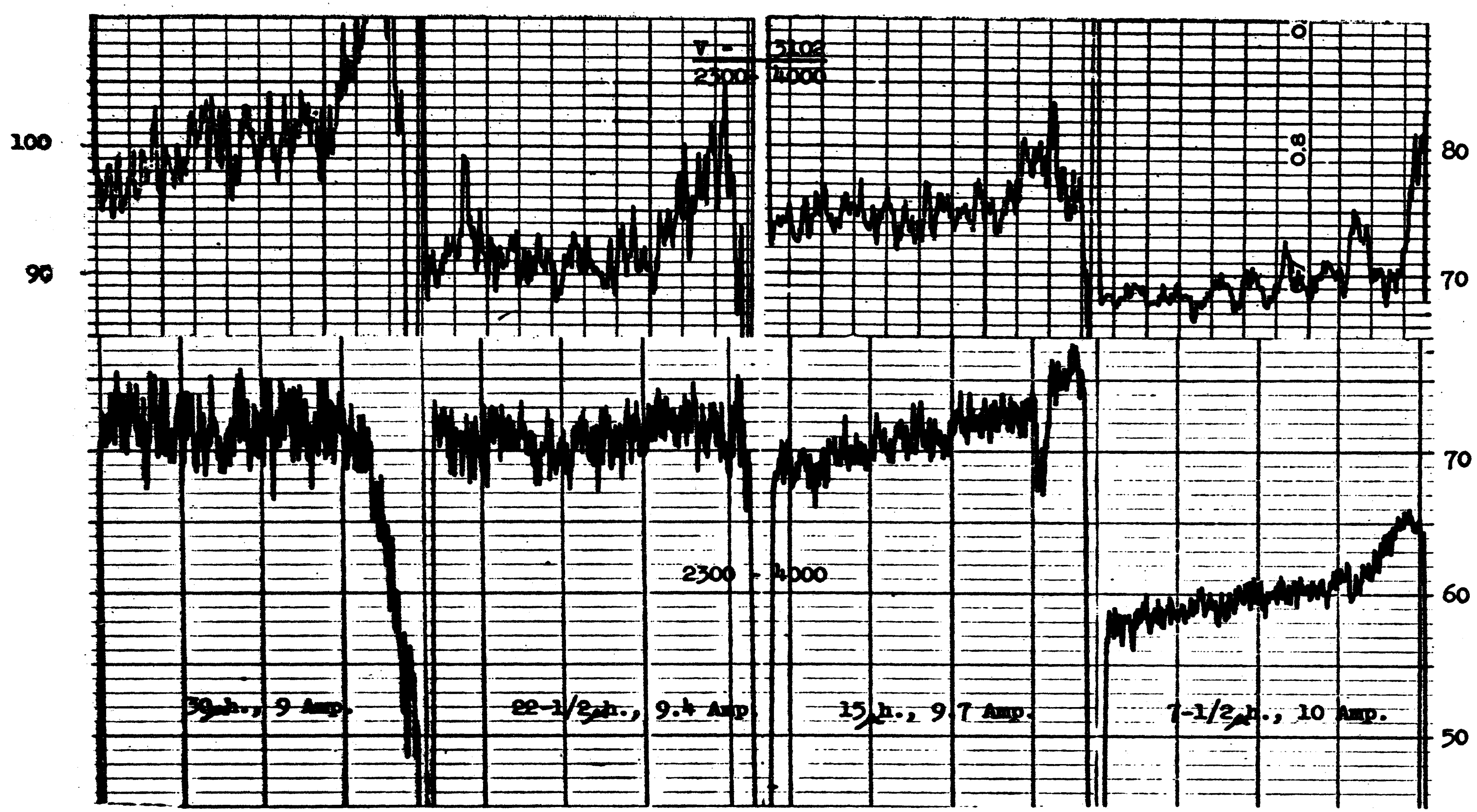

Fig. 7. Ratio and intensity as a function of spark circuit inductance as in Fig. 6, but for point to plane method. Motung tool steel (1.01% V), 1/2" x 1-3/4" flat. Counter electrode 1/4" D, 110° cone, 4 mm spacing, pure Fe.

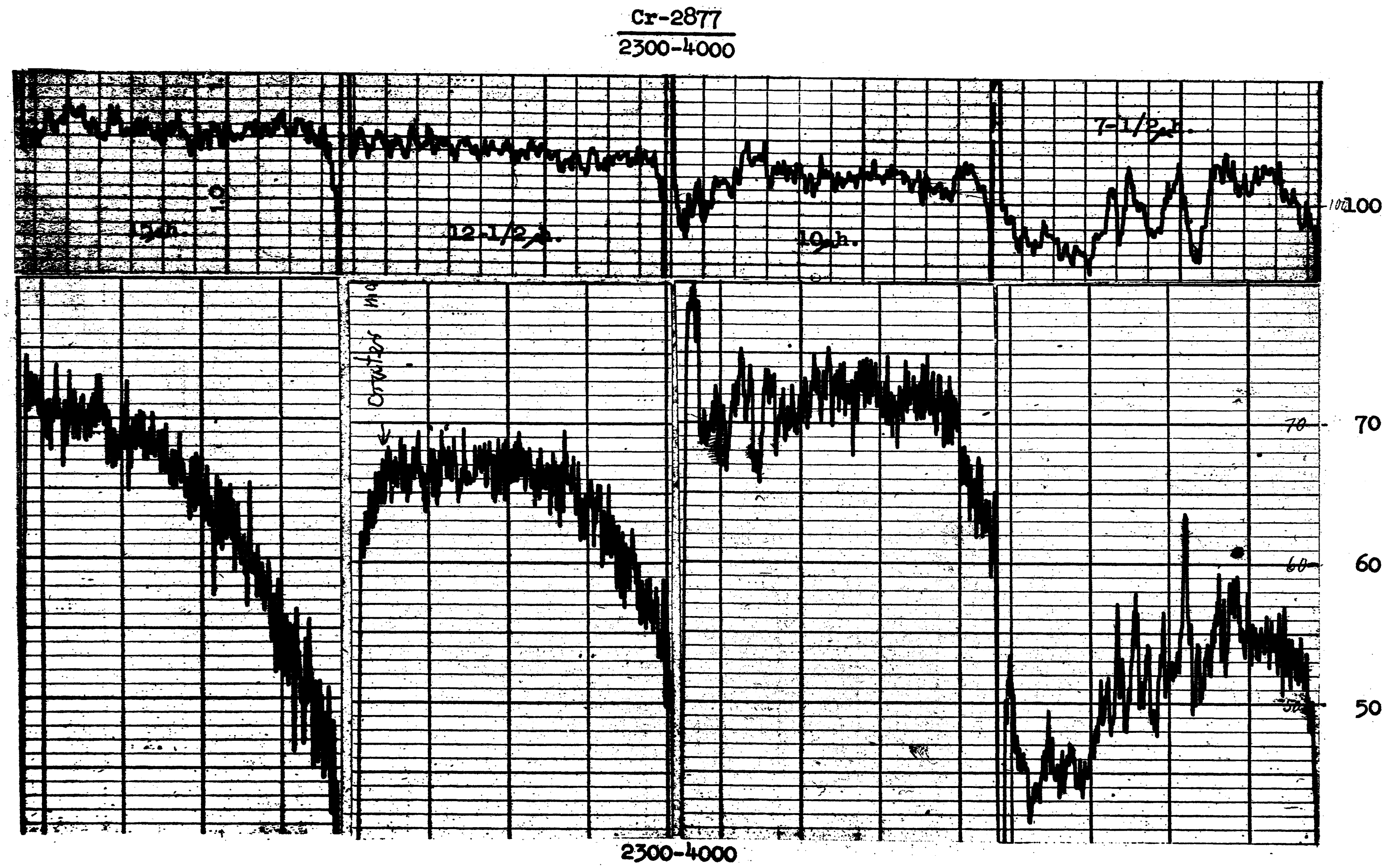

Fig. 8. Ratio and intensity as a function of spark circuit inductance. S IV source with increasing inductance. Stainless steel (18.75% Cr), 7/32" D pins, 140° cone, 4 mm gap.

Cr-2877
2300-4000

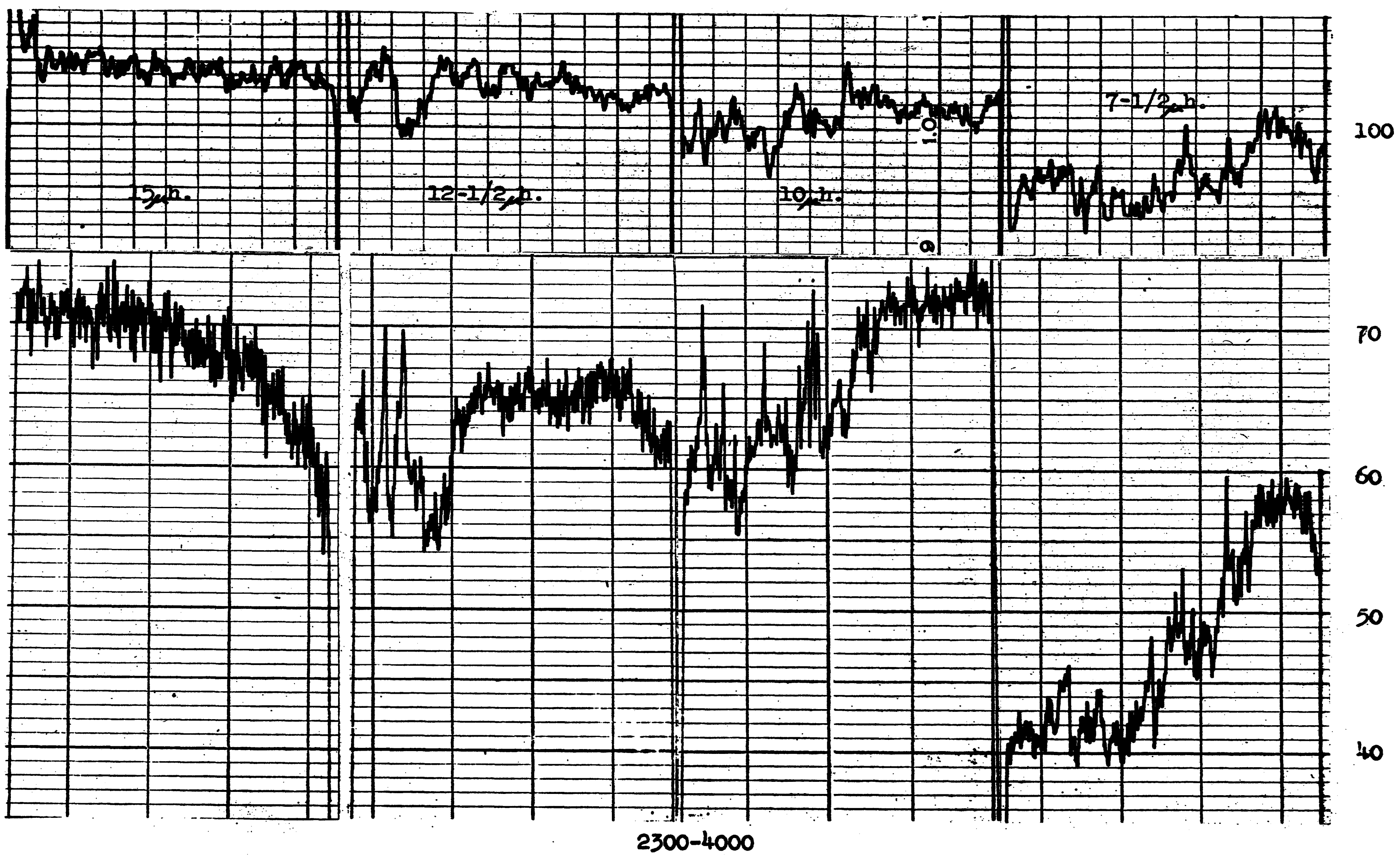

Fig. 9. Ratio and intensity as a function of spark circuit inductance. S IV source with increasing inductance. Stainless steel (18.75% Cr), 7/32" D pins, 130° cone, 4 mm gap.

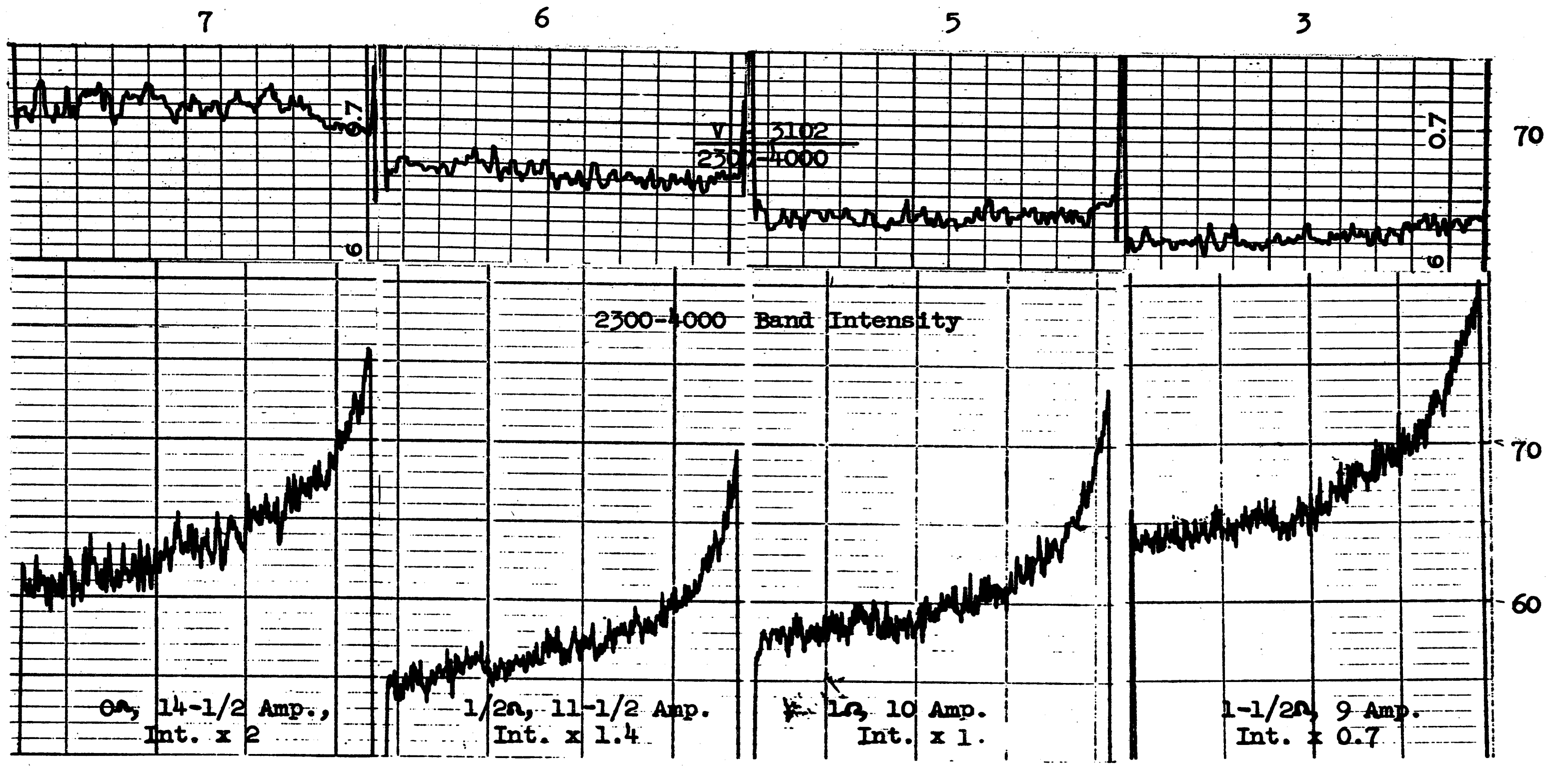

Fig. 10. Ratio and intensity as a function of added spark circuit resistance, otherwise SS-4 source. 130° cone, 4 mm gap, tool steel (1.61% V).

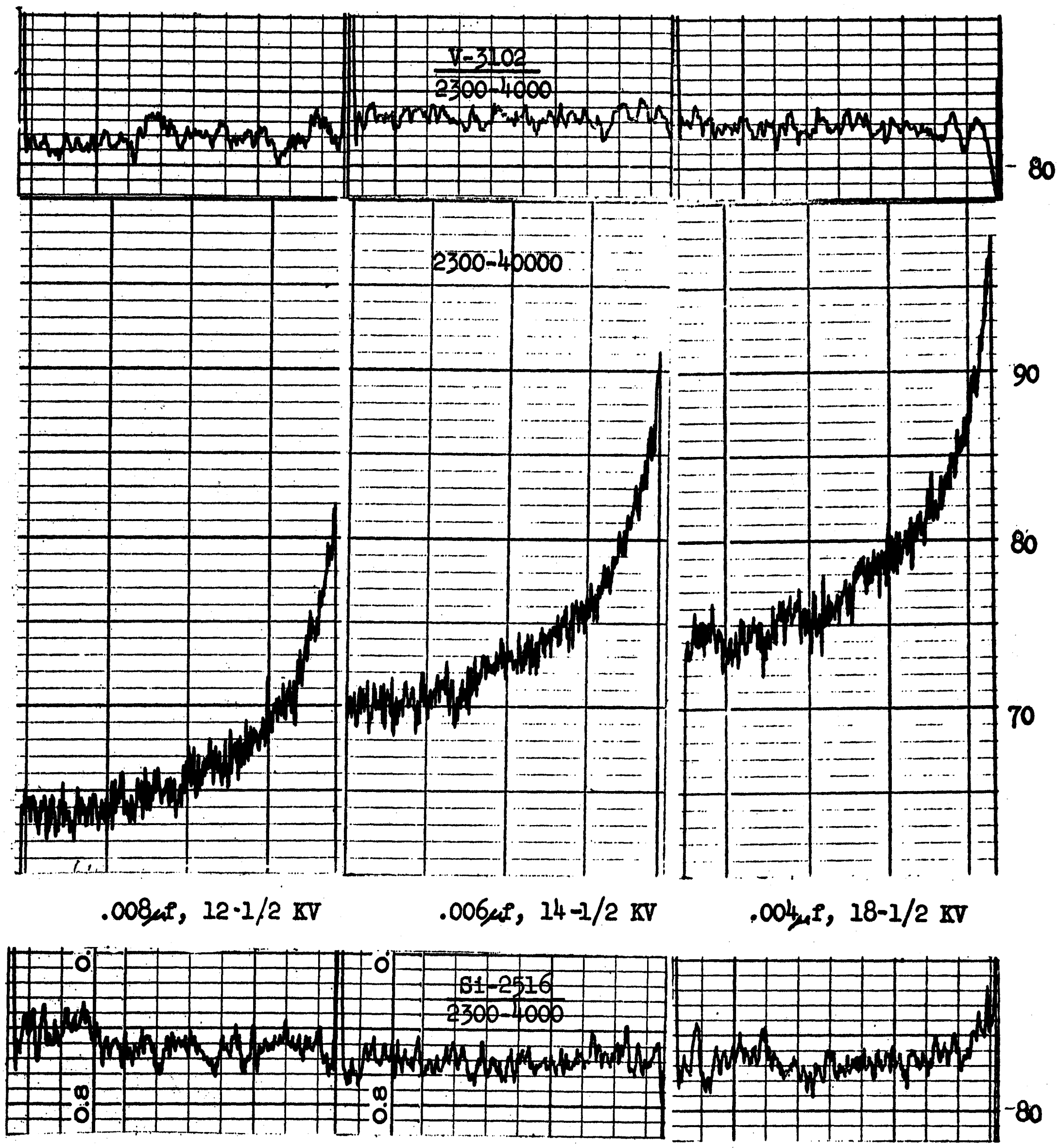

Fig. 11. Effect upon ratio and intensity when C and V are varied to maintain the 10 amperes in the SS-4 source. Tool steel (2.01% V, 0.19% Si). 130° cone, 4 mm, time right to left.

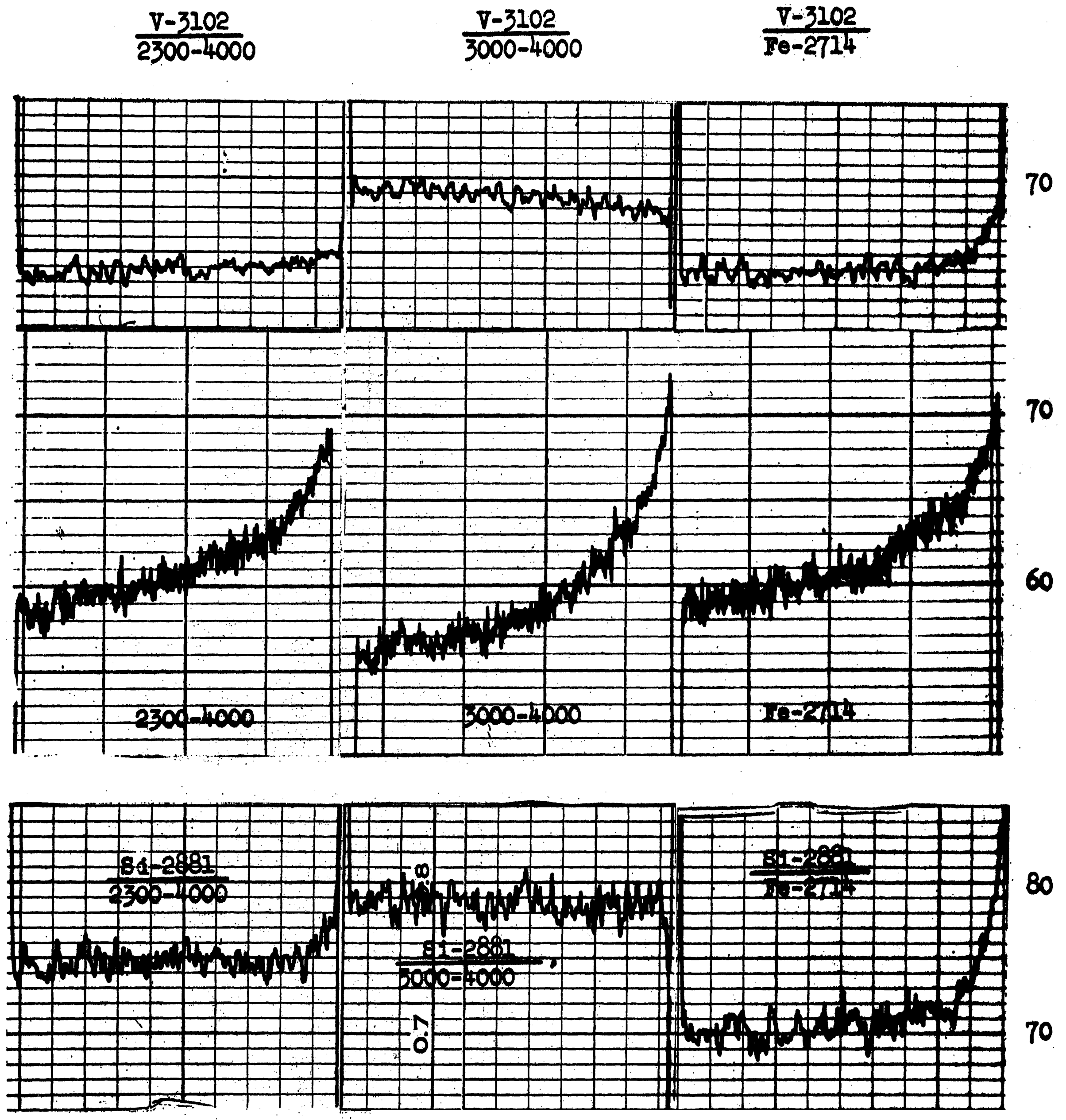

Fig. 12. Vanadium and silicon ratios with the 2300-4000A° band, 3000-4000A° band and the Fe-2714 II line as respective reference signals. The simultaneous reference intensities for vanadium are shown below each ratio, while for silicon only the ratios are given in the bottom records. SS-4 source, 7/32" motung tool steel (1.13% V, 0.32% Si), 130° cone, 4 mm gap. Vanadium MT d-c signal current about 0.2μA at 78 dynode volts, for Si 0.03μA at 86 volts.

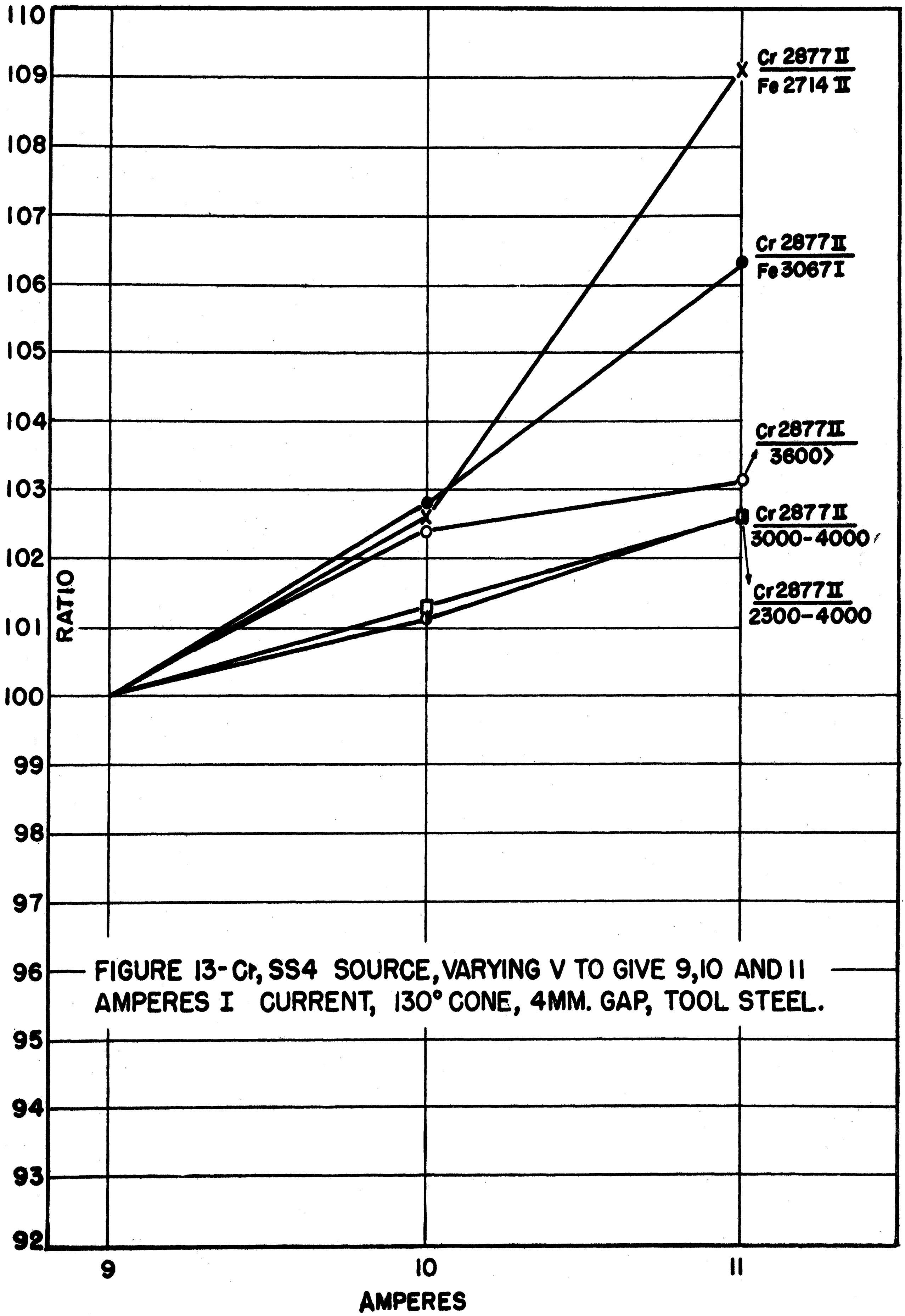

FIGURE 13- Cr, SS4 SOURCE, VARYING V TO GIVE 9,10 AND 11 AMPERES I CURRENT, 130° CONE, 4MM. GAP, TOOL STEEL.

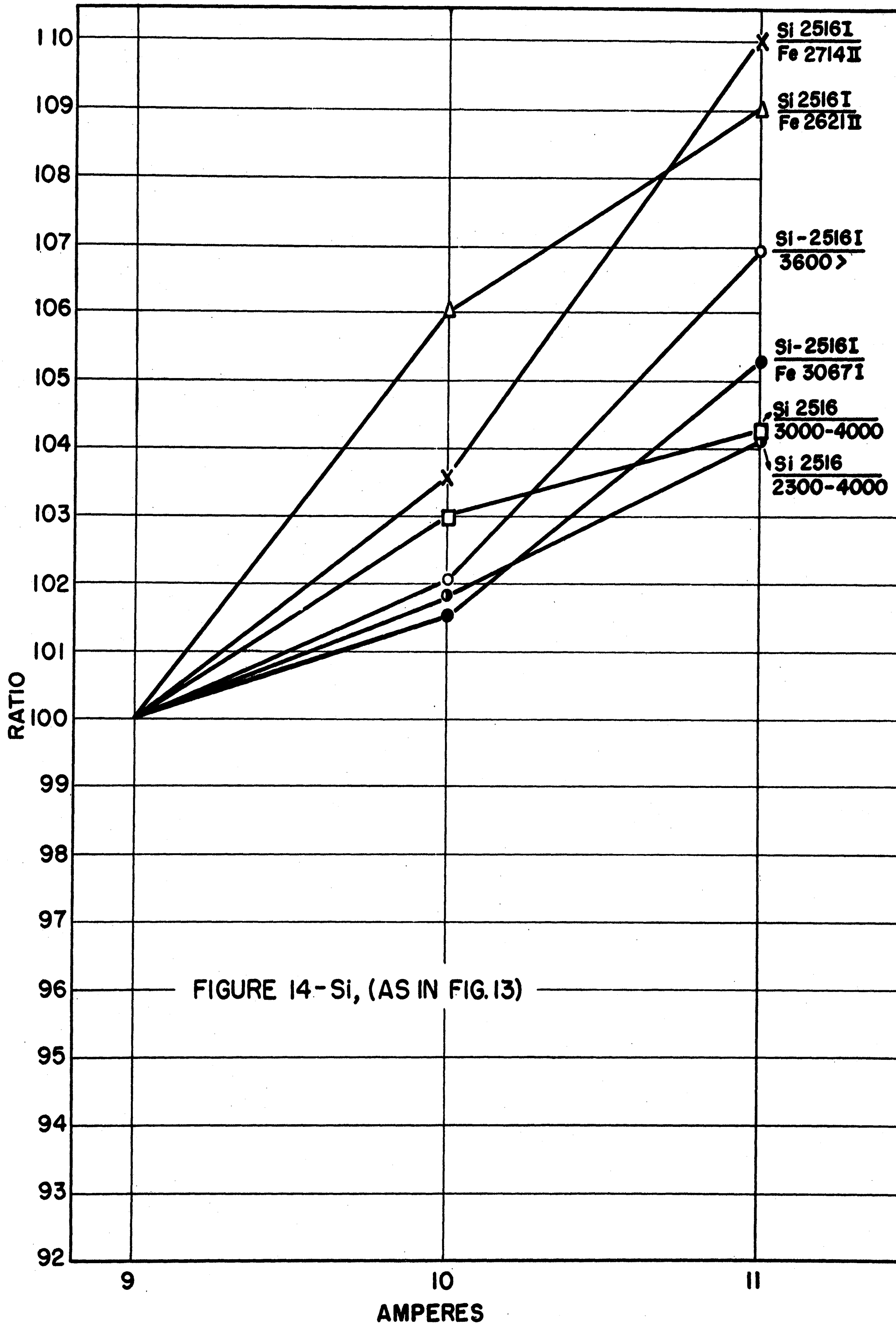

FIGURE 14-Si, (AS IN FIG.13)

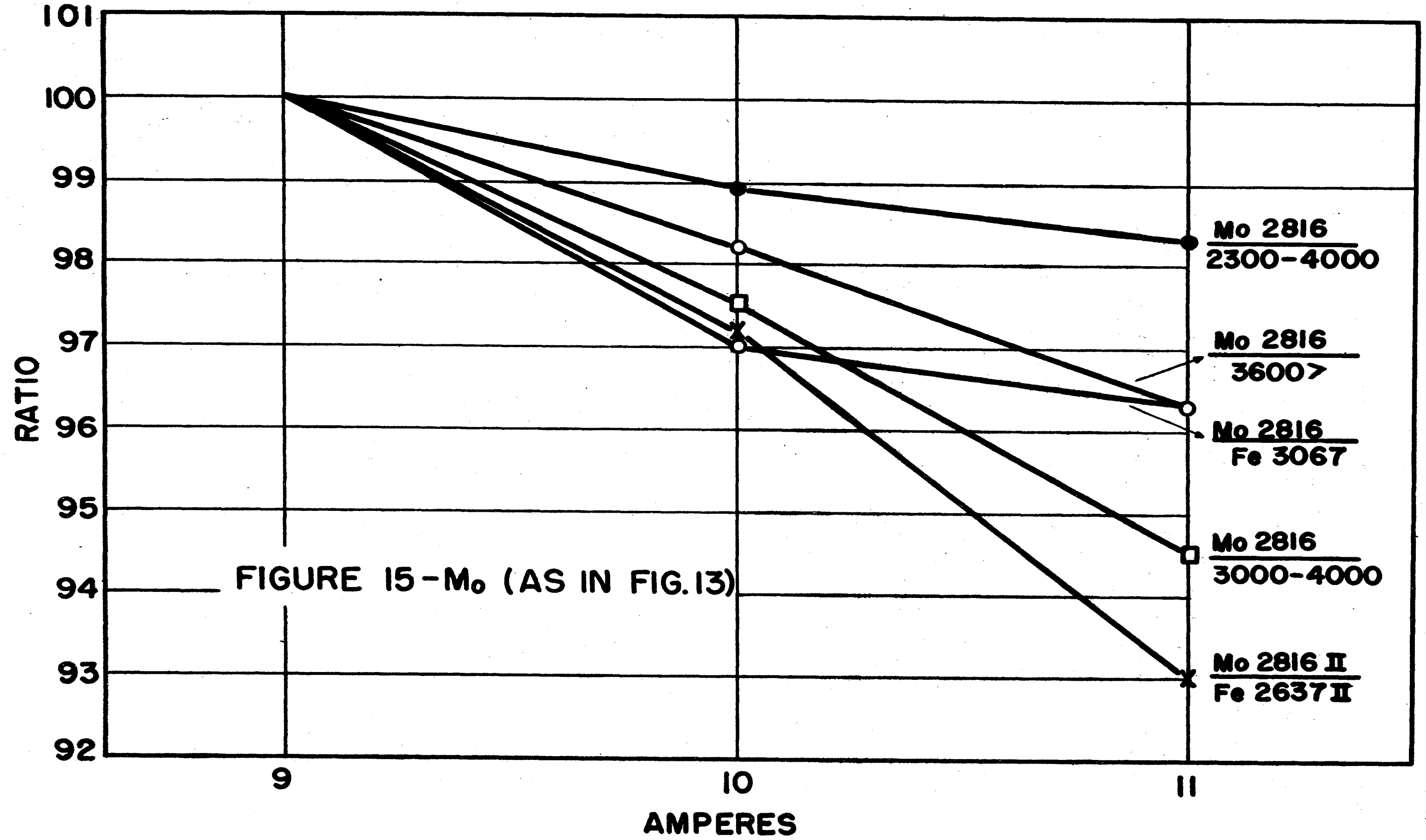

FIGURE 15-Mo (AS IN FIG. 13)